Solution Combustion Synthesis of Metal Nanopowders: Nickel—Reaction Pathways

A. Kumar, E. E. Wolf, and A. S. Mukasyan
Chemical and Biomolecular Engineering, University of Notre Dame, Notre Dame, IN 46556

DOI 10.1002/aic.12416
Published online October 19, 2010 in Wiley Online Library (wileyonlinelibrary.com).

Nanopowders of pure nickel were directly synthesized for the first time by conventional solution combustion synthesis (SCS) method. In this article, a specific reaction pathway is suggested to describe the metallic phase formation during SCS. It is proposed that the exothermic reaction between NH_3 and HNO_3 species formed during the decomposition of glycine and nickel nitrate acts as the source of energy required to achieve the self-sustained reaction regime. A thermodynamic analysis of the combustion synthesis reaction indicates that increasing glycine concentration leads to establishing a hydrogen rich reducing environment in the combustion wave that in turn results in the formation of pure metals and metal alloys. TGA of reaction systems and XRD analysis of products in the quenched combustion wave show that the formation of oxide phases occurs in the reaction front, followed by gradual reduction of oxide to pure metallic phases in the postcombustion zone. A methodology for SCS of pure metals and metal alloys nanoparticles can be inferred from the results presented. © 2010 American Institute of Chemical Engineers *AIChE J,* 57: 2207–2214, 2011
Keywords: combustion synthesis, nanocrystalline materials, metal and alloys, phase transformations

Introduction

Different combustion based techniques are used for the synthesis of various nanomaterials. These methods can be classified based on the physical nature of the reaction media as: (i) flame synthesis, i.e., gas-phase combustion; (ii) heterogeneous condensed phase (solid) combustion; and (iii) solution combustion synthesis (SCS), i.e., the initial reactive media is in an aqueous solution (see recent reviews on these topics[1–3]).

SCS is the most widely used approach for synthesis of high-surface area powders, and many different nanocompounds have been produced by this method.[2,4,5] However, in almost all cases, the powders thus synthesized are oxides. Typically, SCS involves a self-sustained reaction in a solution of metal nitrates and oxygen containing fuels, which can be classified based on the chemical structure of the fuel, i.e., the type of reactive groups (e.g., amino, hydroxyl, and carboxyl) bonded to a hydrocarbon chain. The exothermic reaction between the added fuel and oxygen, formed during decomposition of nitrates, provides conditions for rapid high-temperature reaction. The stoichiometric equilibrium combustion reaction (e.g., by using metal nitrite as an oxidizer and glycine as a fuel) can be described by the following widely accepted scheme:

$$\mathrm{M}^{v}(\mathrm{NO_3})_{v} + \left(\frac{5}{9}v\varphi\right)\mathrm{CH_2NH_2COOH} + v\frac{5}{4}(\varphi-1)\mathrm{O_2} \rightarrow \mathrm{M}^{v}\mathrm{O}_{\frac{v}{2}}(\mathrm{s}) + \left(\frac{10}{9}v\varphi\right)\mathrm{CO_2(g)} + \frac{25}{18}\varphi\mathrm{H_2O(g)} + v\left(\frac{5\varphi+9}{18}\right)\mathrm{N_2(g)} \quad (1)$$

where M^{v} is a v-valent metal and φ is the fuel/oxidizer ratio; $\varphi = 1$ means that the initial mixture does not require

Correspondence concerning this article should be addressed to A. S. Mukasyan at amoukasi@nd.edu

atmospheric oxygen for complete oxidation of the fuel, whereas $\varphi > 1$ (<1) implies fuel-rich (lean) conditions.

According to reaction 1 the final combustion product is a metal oxide. Indeed during the last decade, it has been shown that SCS is an effective and versatile method for synthesis of almost any binary and many complex nano-oxides.[2,4,5] In this work, we investigate if compounds other than oxides, e.g., pure metals or their alloys, can be produced by SCS. This issue was partially addressed experimentally in recent publications by Bhaduri and coworkers.[6,7] However, these authors used complex, microwave induced[6] and mist ultrasonic pyrolysis[7] combustion methods that complicated the search for a simple conventional combustion technique to obtain metals by SCS. Recently, the sol–gel method[8] and conventional solid state combustion synthesis[9] were used to produce metal powders. However, in both cases, an inert atmosphere was used during the combustion reaction, and in the latter case, a postreduction in high pressure hydrogen was used. In the literature, the reaction mechanisms for the formation of non-oxide products during SCS in air have not been investigated. The objective of this work is to propose a single step SCS method to produce pure metals in air. A nickel-based system is used as an example to present experimental and thermodynamics results that pointing to a reaction pathway that can be controlled to produce nanoparticles of other metals and alloys.

Two main reaction modes for SCS are known in the literature: (a) conventional volume combustion synthesis (VCS), which is simple but more difficult to control and could result in a thermal explosion, and (b) the more controllable self-propagating high-temperature synthesis (SHS).[10,11] The former mode involves reaction in a homogeneous aqueous oxidizer–fuel solution that is uniformly heated by a constant temperature heating source (oven, hot plate, etc.). In the latter case, the sample is ignited locally at one point resulting in a combustion wave that propagates in a self-sustained way along the reaction media. In this work, we used both synthesis modes: VSC and SHS. VCS was developed first,[12] and, thus, it is still widely used in many laboratories worldwide.[2,4] The more controllable SHS mode allows one to conduct detailed analysis of the product in the various regions of the combustion front[5–7,10] and thus ascertain the specifics of microstructural transformations in the combustion wave. This article summarizes our studies on the SCS of pure nickel nanosized powders. Special attention was paid to the mechanism of phase formation of products in SHS mode. Based on the results obtained and data reported in the literature, the reaction pathways for SCS of several nono-oxide nanopowders are proposed.

Experimental

The following reagents were used as the precursors: nickel nitrate hexahydrate, $Ni(NO_3)_2{\cdot}6H_2O$, (Alfa Aesar, 98%) and glycine, CH_2NH_2COOH, (Alfa Aesar, 98.5%). The amounts of precursors were calculated on the basis of producing 3 g of pure metal in the product using the stoichiometric Eq. 1. These initially solid reagents were dissolved in the desired ratios in 75 ml of deionized water at room temperature in a beaker of 250 ml capacity and stirred to get a clear homogeneous solution. The resulting solution is then heated over a hot plate (Barnstead Thermolyne, model no: sp 46925 at maximum heating rate setting of 10) in air and atmospheric pressure up to the self-ignition temperature T_{ig}. The combustion mode observed, VCS or SHS, was found to be sensitive to φ.

A high-speed infrared thermal imaging system (SC6000; FLIR Systems, Boston, MA) was used to monitor the temperature–time history of the process. Thermal images and videos can be captured with FLIR's ThermaCAM Researcher software, over several different temperature ranges including temperatures as high as 2000°C. Depending on the frame size and temperature range selected, frame rates above 15,000 fps are achievable. To obtain data on the combustion kinetics of the chemical reactions involved, an SDT-2960 (TA Instruments, New Castle, DE) was used to conduct simultaneous differential thermal analysis (DTA)–thermal gravimetric analysis (TGA) of the mixtures under the following conditions: argon/air gas flow at 80 cc/min and heating rates 5, 10, and 20 K/min in the temperature range 300–1000 K.

The as-synthesized powders and quenched samples were characterized by different methods. BET surface area measurements were carried on a Quantachrome Autosorb-1 unit, using nitrogen as the adsorbent gas. The particles were first outgassed at 473 K until the differential pressure fell below 20 μ Hg per min followed by exposure to N_2 and immersion in a liquid nitrogen bath. X-ray diffraction (XRD) measurements were carried out in air using a Scintag. X-ray diffractometer with Cu-Kα radiation of wavelength 1.54056 Å. Powder microstructures were imaged using Field-Emission scanning electron microscope (SEM), Magellan 400 (FEI) that offers nondestructive imaging capability at a working distance optimized for ultra-high resolution and can produce images magnified to 2500 kx.

The software package "Thermo" was used to perform thermodynamic analysis of the combustion system under adiabatic conditions and to analyze the equilibrium products. This program is based on optimizing the Gibbs free energy of multiphase and multicomponant systems. It assumes gases to be ideal and condensed phases to be completely immiscible (see details in Ref. 13).

Results and Discussion

The temperature–time profile for VSC mode in nickel nitrate hexahydrate–glycine system is shown in Figure 1a, as recorded by the FLIR-camera. It can be seen that after the water evaporated, the temperature of the formed sol–gel viscous media increases, achieving an ignition point $T_{ig} \sim 517$ K, at which the reaction spontaneously initiates and the temperature rapidly increases up to its maximum value ($T_m \sim 650$ K). Figure 1b shows the temperature profile of SHS mode in this system. The solution is ignited at one end and then it self-propagates as a combustion wave along the reaction media. It can be seen that the SHS process is characterized by two temperature peaks at about 750 and 800 K.

These experiments raised the following questions: what factors determine the ignition temperature for the VSC mode, and what processes lead to the observed maximum temperatures during the SHS mode? Answering such questions, one may control the synthesis process and the composition of the desired product. In our previous work,[14] where the iron nitrate–glycine system was investigated for VCS mode, it was suggested that the ignition temperature may be

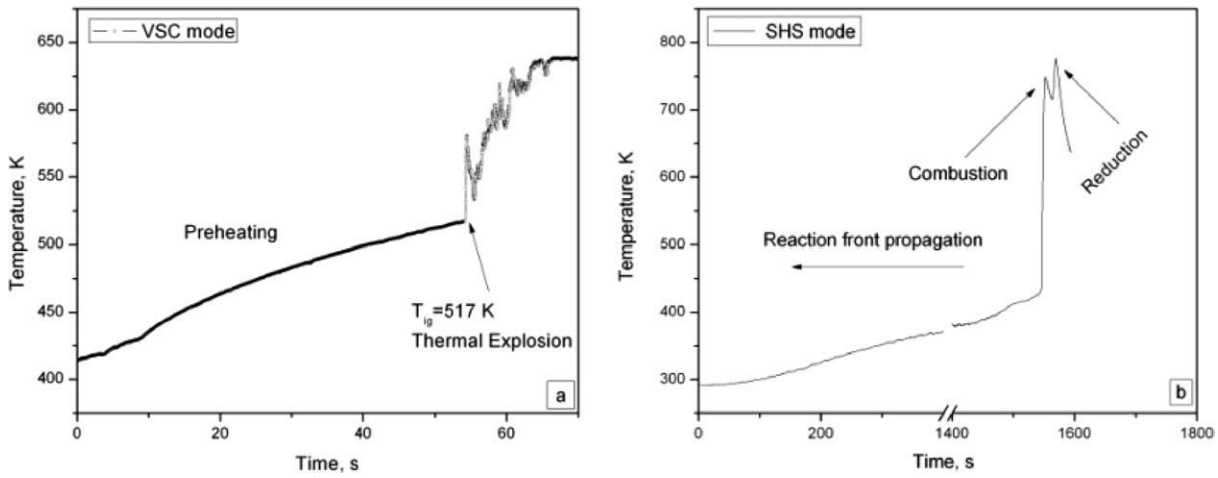

Figure 1. Temperature profiles for SCS in nickel nitrate hexahydrate–glycine (φ = 1.75) system: (a) VSC; (b) SHS.

related to the specific decomposition temperature of one of the reagents in the solution. The results below, along with literature results from others, allow us to give deeper elaboration of such conceptual statement.

Typical TGA curves for decomposition of precursors (glycine: curve 1; nickel hexahydrate: curve 2), obtained under conditions described in the Experimental section, are shown in Figure 2a. It can be seen that this process is characterized by a sharp weight loss starting at 513 K followed by a gradual weight change starting at ~562 K until all glycine is reacted. Nickel nitrate decomposition shows a gradual weight loss until 452 K followed by a second region that stabilizes at ~25% weight change, corresponding to nickel oxide (NiO) formation. The DTA results (not shown) for nickel nitrate reveals a large exotherm at ~500 K and a smaller one at ~625 K.

These results are similar to recent TGA–Fourier transformation infrared (FTIR) analyses of the thermal decomposition of the pure glycine in inert atmosphere by Li et al.,[15] showing that this process can be divided into three stages. The first stage was a sharp weight loss of ~55% that took place in the temperature range of 510–585 K, and it corresponded to the formation of NH_3, H_2O, and CO_2 gaseous products. The maximum release rate for both NH_3 and H_2O was reached at ~560 K, whereas for CO_2 it is at a higher temperature of ~580 K. These authors suggested that the deamination (Eq. 2) and dehydration (Eq. 3) reactions are responsible for glycine decomposition in the first stage (510–585 K), according to the following scheme:

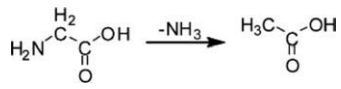

(2)

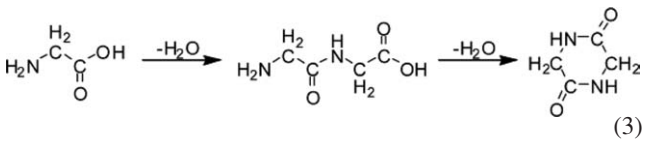

(3)

This stage was followed by two relatively slow weight loss stages at 585–730 K and 730–1000 K. In the former temperature range, HNCO and CO were the gas phase products; whereas in the latter, HCN is the main gaseous species. The intermediate of

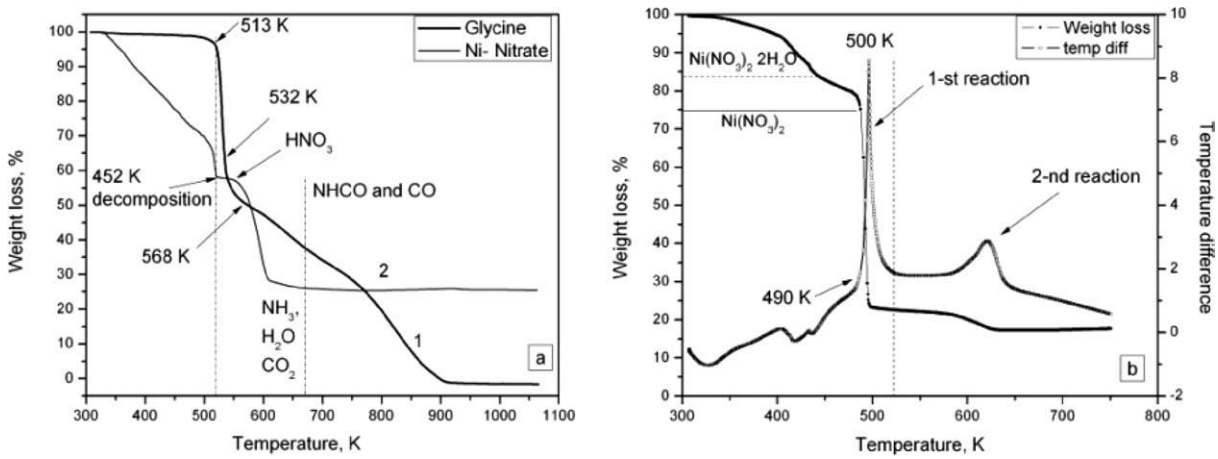

Figure 2. (a) Typical TGA profile during thermal decompositions in air of (1) glycine and (2) nickel nitrate hexahydrate; (b) DTA–TGA data during reaction in glycine–nickel nitrate hexahydrate (φ = 1.75) aqueous solution.

Table 1. Steps for Nickel Nitrate Decomposition

Reactions/Steps	Temperature (K)	Experimental, Δm (%)
Dehydration		
$Ni(NO_3)_2{\cdot}6H_2O \rightarrow Ni(NO_3)_2{\cdot}4H_2O + 2H_2O$	316	12.3
$Ni(NO_3)_2{\cdot}4H_2O \rightarrow Ni(NO_3)_2{\cdot}2H_2O + 2H_2O$	353	24.8
Partial decomposition steps		
$Ni(NO_3)_2{\cdot}2H_2O \rightarrow Ni(NO_3){\cdot}(OH)_2\ H_2O + NO_2$	418	40.6
$Ni(NO_3){\cdot}(OH)_2{\cdot}H_2O \rightarrow Ni(NO_3){\cdot}(OH)_{1.5}\ {\cdot}O_{0.25}{\cdot}H_2O + 0.25H_2O$	463	42.0
Decomposition		
$Ni(NO_3){\cdot}(OH)_{2.5}\ {\cdot}O_{0.25}{\cdot}H_2O \rightarrow 0.5\ Ni_2O_3 + HNO_2 + 1.25H_2O$	523	71.8
Oxide decomposition to NiO		
$3Ni_2O_3 \rightarrow 2Ni_3O_4 + 0.5O_2$	523	72.2
$Ni_3O_4 \rightarrow 3NiO + 0.5O_2$	573	74.0

2,5-piperazinedione (Eq. 4) provided a suitable explanation for their formation according to the following reactions:

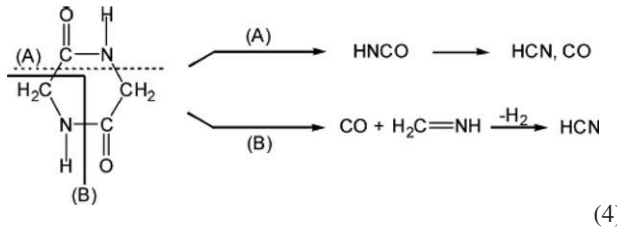

(4)

Summarizing the above results from Li et al.[15] for glycine decomposition, one can conclude that: (i) glycine decomposition starts at ~515 K; (ii) the main product on the first stage of decomposition is NH_3; (iii) CO and HNCO are decomposition products in the temperature range 585–730 K.

All the above stages can also be seen for the glycine decomposition; TGA results are obtained in this work under similar heating rate (20 K/min) but in air instead of N_2 as in Li et al.'s work (see curve 1 Figure 2a). However there is a difference, as the overall weight loss for glycine pyrolysis in nitrogen was reported to be 85.5% at ~1000 K, whereas in air it is 100%. This effect can be attributed to the oxidation of the residuals—by oxygen in air. Indeed, two additional exothermic peaks (not shown in the figure) were observed in our work at temperatures >800 K that leads to complete weight loss of the sample.

The decomposition of nickel nitrate hexahydrate used in this work as nickel-containing precursor is also shown in Figure 2a, curve 2. In general, it is an endothermic process leading to the formation of NiO. The following thermal decomposition route in air (Table 1) was recently suggested for this compound based on advanced TGA.[16] The first stage, occurring in the temperature range 310–350 K, involves just water evaporation from the solution and dehydration. The second stage, at 420–460 K, consists of partial decomposition steps of the precursor with formation of $Ni(NiO_3)(OH)_x{\cdot}H_2O$ species and release of water. The third stage, referred as total decomposition, starts at ~525 K and can be described as follows:

$$Ni(NO_3)(OH)_{2.5}O_{0.25} \cdot H_2O \rightarrow 0.5Ni_2O_3 + HNO_3 + 1.25H_2O \quad (5)$$

It is important to note that according to Eq. 5, HNO_3 is the main gas phase product that forms in this stage. The final stage is Ni_2O_3 decomposition to NiO occurring at 523–573K (Table 1). Our TGA results obtained under similar conditions (Figure 2a: curve 2) show regions of weight changes that are in a good agreement with the suggested decomposition mechanism. Comparative analysis of TGA curves for glycine and nickel nitrate hexahydrate decomposition indicates that these reactions occur approximately in the same temperature range of 510–620 K from which it can be inferred that the decomposition species are gaseous HNO_3 and NH_3. If so they could be present simultaneously during the VSC in metal nitrate–glycine system.

The stoichiometric reaction in the solution of the dehydrated precursor and glycine used during CS can be represented as follows:

$$Ni(NO_3)_2 + \frac{10}{9}\varphi CH_2NH_2COOH + \left[\frac{5}{2}(\varphi - 1)\right]O_2 \rightarrow NiO + \frac{20}{9}\varphi CO_2 + \frac{25}{9}\varphi H_2O + \left(\frac{5\varphi + 9}{9}\right)N_2 \quad (6)$$

The DTA–TGA results obtained for this reactive solution during preheating in flowing air at a heating rate 20 K/min is shown in Figure 2b. A large exothermic peak is observed at T ~500 K along with a significant change in weight, similar to results found for the precursor decomposition (compare Figures 2a and b). These observations allow us to infer that HNO_3 and NH_3 are the main gas products of the precursors decomposition (nitrate and glycine, respectively), and during solution combustion they are mixed in one volume and, therefore, they can react with each other.

To further analyze HNO_3 and NH_3 reaction, thermodynamic calculations were performed to estimate the adiabatic combustion temperature and gas phase compositions. The calculations show that HNO_3 and NH_3 mixture is extremely exothermic. The dependences of the adiabatic combustion temperature (see Ref. 17) and equilibrium products, as a function of NH_3:HNO_3 mole ratio, are presented in Table 2 and Figure 3. Indeed, it can be seen that this system reacts resulting in high temperatures and H_2O, N_2, and H_2 as the main equilibrium products. Thus, it can be inferred that the gas phase combustion reaction between HNO_3 and NH_3 species is the driving force for the solution combustion process between nitrate precursors and glycine.

However, the nickel nitrate hexahydrate–glycine solution contains at least 5.5 molecules of H_2O of hydration, and one mole of NiO phase. Taking this into account one may calculate the adiabatic combustion temperature in the following

Table 2. Adiabatic Combustion Temperature (T_{ad}) in NH_3:HNO_3 System as a Function of NH_3:HNO_3 Mole Ratio

Mole ratio	1	2	3	4	5
T_{ad} (K)	2300	2580	2050	1600	1300

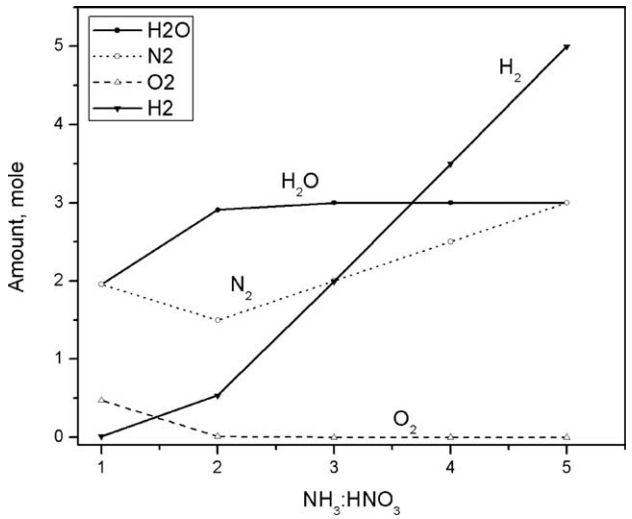

Figure 3. Equilibrium combustion products in NH_3:HNO_3 system.

system HNO_3: x NH_3:5.5·H_2O:NiO as a function of x, i.e., as a function of the NH_3 to HNO_3 molar ratio. Figures 4a, b show the results from calculations of the adiabatic combustion temperature and equilibrium products as a function of x (except the amount of H_2O, which increases monotonically from 7.5 to 9.5 moles when "x" increases from 1 to 3.5). It can be seen that the adiabatic combustion temperature is in the range of 450–900 K and is maximum at $x = 2$. Three regions that have qualitatively different equilibrium products can be outlined. At lower values of x, <1.5, the only solid state product formed is NiO along with oxygen, and at higher values of x, >2.5, the only solid state product is nickel, whereas H_2 defines the reducing gas phase composition. Some intermediate zone also exists, where both NiO and nickel are equilibrium products. Thus according to these calculations, it can be concluded that by increasing the amount of fuel in the reactive solution, one may increase the amount of NH_3 on the first stage of combustion reaction, thus, changing the solid state products from NiO through NiO + Nickel mixture to Nickel.

It is worth noting that when considering only the first stage (520–650 K) of glycine decomposition, the main gas phase product of pyrolysis is NH_3. Li et al.[15] have also shown that at higher temperatures, HNC + CO and HCN become the main species of glycine decomposition, which, of course, contributes to the overall mechanism of solution combustion reaction. Indeed in this stage, carbon-containing phases (HCN, CO, C) are the reducing elements for NiO. If the initial composition contains enough fuel, which in the first combustion stage provides sufficient amount of hydrogen to reduce NiO to nickel, formation of CO may also prevent the secondary oxidation of pure nickel to NiO by interaction with oxygen in air in postcombustion zone.

The above discussion suggests that the self-ignition temperature, which is the main characteristic for the VSC mode, is related to the decomposition temperatures of the precursor and fuel that occur in the range 510–515 K. The good agreement of this prediction with experiments (Figure 1a) allows us to propose that the highly exothermic reaction between the glycine and nitrate decomposition products, i.e., NH_3 and HNO_3, is primarily responsible for the self-sustained nature of the process. Thus, one can expect that on the first stage of the SCS process nickel nitrate hexahydrate self-decomposes to NiO; in excess of fuel, it provides the reducing atmosphere (H_2, CO), which should lead to formation of pure nickel (Figure 4b).

Typical SEM images of the microstructure of as-synthesized pure nickel are shown in Figures 5a, b. It can be seen that this product has a highly porous structure with tightly agglomerated nanocrystallites with individual size well below 50 nm. Figure 5c shows the XRD patterns obtained for the final products in $Ni(NO_3)_2$–$\varphi C_2H_5NO_2$ system as a function of fuel/oxidizer ratio in the range of φ from 0 to 1.25. It can be seen that for $\varphi = 0$, i.e., the case of simple nickel nitrate decomposition, the final product involves only NiO. Increasing φ, as predicted above, leads to the increased

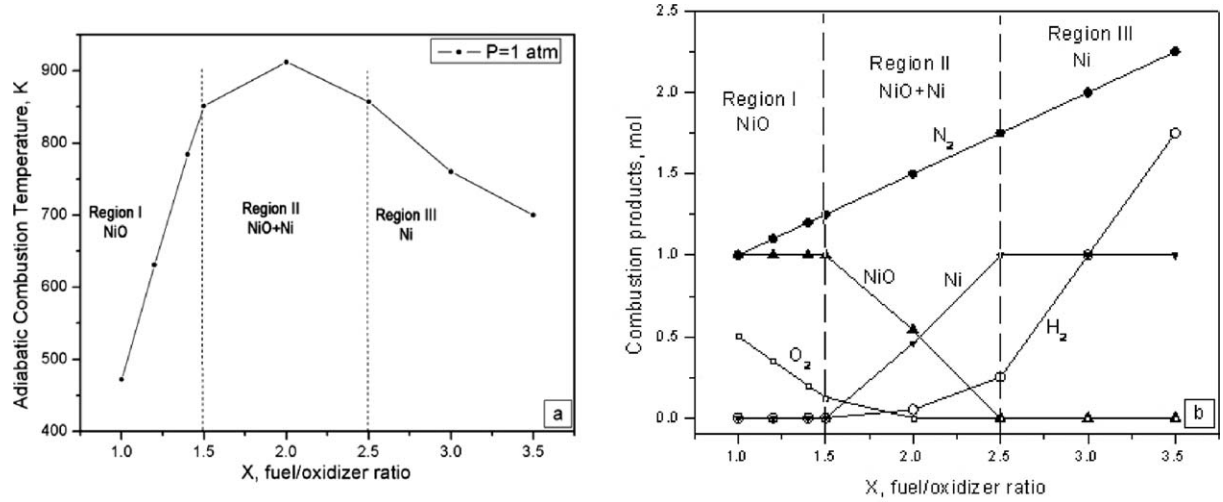

Figure 4. Thermodynamic characteristics of HNO_3: x·NH_3:5.5·H_2O:NiO system: (a) adiabatic combustion temperature; (b) equilibrium products.

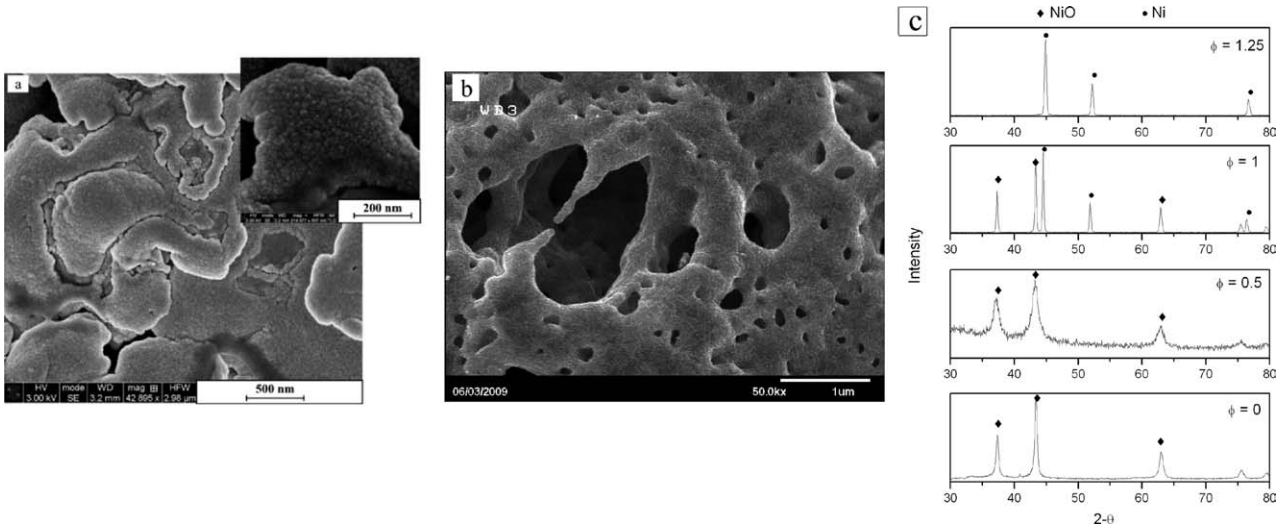

Figure 5. Typical microstructures (a) and (b); XRD patterns (c) of SCS products in glycine–nickel nitrate system.

amount of nickel phase and pure metal was synthesized when $\varphi = 1.25$ by both VSC and SHS modes.

As it was mentioned previously, it is difficult to investigate the sequence of phase transformations during VCS due to the explosive nature of the reaction. Careful examination of a typical temperature–time profile of the combustion wave in SHS mode shows the existence of two temperature peaks (Figure 1b). In turn, relatively slow velocities of the reaction front propagation (~5 mm/s) allow one to quench the process. Figure 6 shows results of the XRD analysis of the combustion products for a nickel nitrate–glycine solution with $\varphi = 1.75$ prepared by SHS and quenched before (a) and after (b) the appearance of the second temperature peak. It can be seen that the products formed in the combustion front (after the first peak in Figure 1b) consist primarily of NiO phase. After the second reaction, only pure nickel phase was detected. It is interesting that two peaks were also observed during DTA of the same composition (Figure 2b). These results provide additional evidence for the proposed reaction pathway for pure metal formation during solution combustion (SC) in this system.

The Kissinger[18] method has been used to determine the activation energy of the reactions in nickel nitrate hexahydrate–glycine system. According to this approach, the reaction kinetics is described as follows:

$$\frac{dx}{dt} = A(1-x)^n \ \exp(-E/RT) \tag{7}$$

where dx/dt is the reaction rate, A is the frequency factor, x is the fraction reacted, n is reaction order, E_a is the activation energy, and T is the temperature in Kelvin. If the reaction is accompanied by a rise in temperature, then the reaction rate, dx/dt, will rise to a maximum value and return to zero once the limiting reactant is depleted. This maximum occurs when the time derivative of the reaction rate is zero. Through differentiation and setting the result equal to zero, the Kissinger equation is obtained:

$$\frac{E_a \beta}{RT_p^2} = An(1-x)_p^{n-1} e^{-\frac{E_a}{RT_p}} \tag{8}$$

where β is the heating rate, which is expressed as $\beta = dT/dt$, and T_p is the temperature at which the maximum rate occurs. Taking the logarithm of the above equation, one obtains:

$$-\ln\left(\frac{\beta}{T_p^2}\right) = -\ln\left(\frac{AR}{E_a}\right) + \left(\frac{E_a}{R}\right)\left(\frac{1}{T_p}\right) \tag{9}$$

Thus, the activation energy, E_a can be computed by plotting (β/T_p^2) as a function of $1/T_p$, where T_p is the peak temperature. The reactive solution with $\varphi = 1.75$ was analyzed at three different heating rates of 5, 10, and 20 K/min. Figure 7 shows Arrhenius type dependencies plotted for the first reaction (curve 1) and the second (curve 2) reaction. Activation energy for reaction 1 appears to be $E_1 = 123 \pm 10$ kJ/

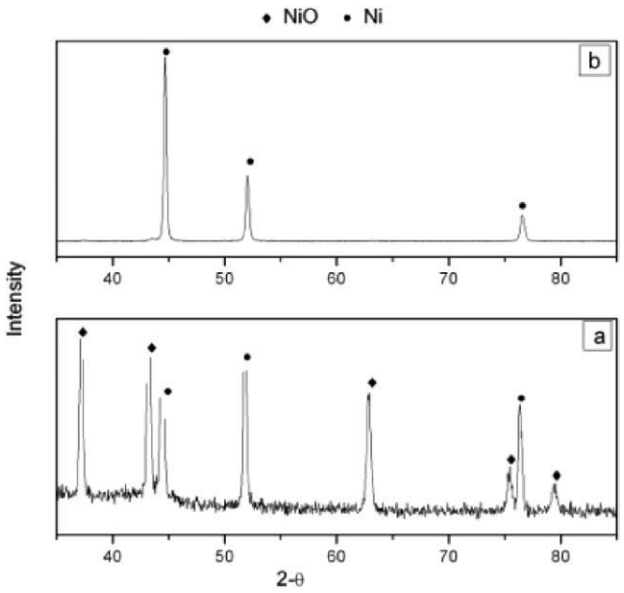

Figure 6. XRD patters for the products formed after first (a) and second (b) reactions in the combustion wave of glycine–nickel nitrate system.

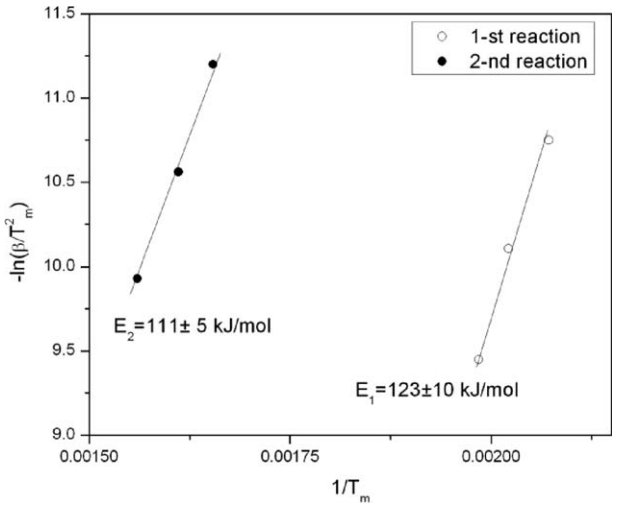

Figure 7. Arrhenius plots for first (curve 1) and second (curve 2) combustion reactions in nickel nitrate hexahydrate–CH_2NH_2COOH system.

mol, whereas for the metal reduction reaction is $E_2 = 111 \pm 5$ kJ/mol.

The kinetics of the reaction between NH_3 and NHO_3 (1st combustion reaction) has not been investigated separately, but only as a part of the thermal decomposition of ammonium dinitramide[19] (NH_4^+ $N(NO_2)_2^-$). However, to our knowledge, no data on the activation energy of this reaction have been reported in literature. The kinetics of NiO reduction by hydrogen has been studied over a wide range of temperatures between 430 and 1300 K under different reaction conditions. A review[20] on this topic concluded that the values of the apparent activation energies could be divided into two categories: (i) corresponding to conditions of gas-phase mass transfer limitations (17–22 kJ/mole) and (ii) corresponding to reaction kinetics limitations (98–133 kJ/mole). In our case, it can be seen that the second reaction that corresponds to reduction of NiO has $E_a \sim 110$ kJ/mole, which is in a good agreement with a kinetic controlled chemical reaction.

Concluding Remarks

Thus, it is proposed that the self-sustained propagation of a combustion wave in the sol–gel media of nickel nitrate and glycine occurs via the reaction between decomposition products of glycine and nitrate. Excess glycine (fuel) provides a hydrogen reduction atmosphere in the reaction front, leading to the formation of pure metal in the postcombustion zone. The suggested mechanism explains all the observed combustion and TGA results in this work and is in agreement with results from others.[15,16] It is more important that based on this mechanism a methodology for SCS of pure metals and metal alloys can be suggested. It follows that the necessary condition for SC of pure metals in oxidizer–glycine system is the property of the oxidizer (e.g., metal nitrate) to decompose with formation of HNO_3. Based on this methodology, pure Cu nanopowders and its alloy with nickel were also synthesized and some other metals such as Co and Fe are under investigation. The specifics of the combustion reactions and phase transformations that take place during SCS of these nanopowders are currently under investigation.

Metal nanoparticles are known for their potential application in various fields, such as: catalysis, pigments, electronic and magnetic materials, drug delivery, etc. In our laboratory, these materials are being prepared for their specific use in catalytic hydrogen generation from light alcohols. Nickel-based catalysts are widely used in various processes including steam reforming, hydrogenation, and decomposition reactions. Similarly, Cu in presence of zinc is known to be active for methanol reforming reactions. In our previous works,[21,22] we showed that catalysts prepared by SCS were extremely active at low temperatures for hydrogen production from oxidative reforming of methanol. Currently, we are applying the SCS approach for preparation of wide spectra of complex catalysts for other catalytic reactions, including oxidative reforming of ethanol and different bio fuels.

Acknowledgment

We gratefully acknowledge funding from NSF Grant 0730190 to support this work. This work was also partially supported by Notre Dame Integrated Imaging Facility.

Literature Cited

1. Roth P. Particle synthesis in flames. *Proc Combust Inst*. 2007;31:1773–1788.
2. Aruna ST, Mukasyan AS. Combustion synthesis and nanomaterials. *Curr Opin Solid State Mater Sci*. 2008;12:44–50.
3. Merzhanov AG, Borovinskaya IP, Sytchev AE. *SHS of nanopowders*. In: Baumard J-F, editor. *Lessons in Nanotechnology from Traditional Materials to Advanced Ceramics*. Dijon, France: Techna Group Srl, 2005:1–27.
4. Patil KC, Hegde MS, Tanu R, Aruna ST. *Chemistry of Nanocrystalline Oxide Materials: Combustion Synthesis, Properties and Applications*. Singapore: World Scientific Publishing, 2008.
5. Mukasyan AS, Epstein P, Dinka P. Solution combustion synthesis of nanomaterials. *Proc Combust Inst*. 2007;31:1789–1795.
6. Choong-Hwan J, Jalota S, Bhaduri SB. Quantitative effects of fuel on the synthesis of Ni/NiO particles using a microwave-induced solution combustion synthesis in air atmosphere. *Mater Lett*. 2005;59:2426–2432.
7. Choong-Hwan J, Hee-Gyoun L;Chan-Joong K, Bhaduri SB. Synthesis of Cu–Ni alloy powder directly from metal salts solution. *J Nanopart Res*. 2003;5:383–388.
8. Jiang Y, Yang S, Hua Z, Huang, H. Sol–gel autocombustion synthesis of metals and metal alloys. *Angew Chem Int Ed Engl*. 2009;48:8529–8531.
9. Nersisyan HH, Won H, Won CW, Cho KC. Combustion synthesis of nanostructured tungsten and its morphological study. *Powder Technol*. 2009;189:422–425.
10. Patil KC, Aruna ST, Mimani T. Combustion synthesis: an update. *Curr Opin Solid State Mater Sci*. 2002;6:507–512.
11. Mukasyan AS, Dinka P. Novel approaches to solution-combustion synthesis of nanomaterials. *Int J Self-Prop High-Temp Synth*. 2007;16:23–35.
12. Kingsley JJ, Patil KC. A novel combustion process for the synthesis of fine particle α-alumina and related oxide materials. *Mater Lett*. 1988;6:427–432.
13. Shiryaev AA. Distinctive features of thermodynamic analysis in SHS investigations. *J Eng Phys Thermophys*. 1993;65:957–962.
14. Deshpande K, Mukasyan AM, Varma A. Direct synthesis of iron oxide nanopowders by the combustion approach: reaction mechanism and properties. *Chem Mater*. 2004;16:4896–4904.
15. Li J, Zhiyong W, Xi Y, Ling H, Yuwen L, Cunxin WJ. Evaluate the pyrolysis pathway of glycine and glycylglycine by TG–FTIR. *J Anal Appl Pyrolysis*. 2007;80:247–253.

16. Brockner W, Ehrhardt C, Gjikaj M. Thermal decomposition of nickel nitrate hexahydrate, $Ni(NO_3)_2{\cdot}6H_2O$, in comparison to $Co(NO_3)_2{\cdot}6H_2O$ and $Ca(NO_3)_2{\cdot}4H_2O$. *Thermochim Acta*. 2007;456:64–68.
17. Zeldovich YB, Barenblatt GI, Librovich VB, Makhviladze GM. *The Mathematical Theory of Combustion and Explosions*. New York and London: Consultants Bureau, 1985.
18. Kissinger HE. Reaction kinetics in differential thermal analysis. *Anal Chem*. 1957;29:1702–1706.
19. Yang R, Thakre P, Yang V. Thermal decomposition and combustion of ammonium dinitramide (Review). *Comb Expl shock waves*. 2005;41:657–679.
20. Richardson JT, Scates R, Twigg MV. X-ray diffraction study of nickel oxide reduction by hydrogen. *Appl Catal A: Gen*. 2003;246:137–150.
21. Schuyten S, Dinka P, Mukasyan AS, Wolf EE. A novel combustion synthesis preparation of $CuO/ZnO/ZrO_2/Pd$ for oxidative hydrogen production from methanol. *Catal Lett*. 2008;121:189–198.
22. Kumar A, Mukasyan AS, Wolf EE. Impregnated layer combustion synthesis method for preparation of multicomponent catalysts for the production of hydrogen from oxidative reforming of methanol. *Appl catal A: Gen*. 2010;372:175–183.

Manuscript received Apr. 21, 2010, and revision received Aug. 15, 2010.